2017

Transport of Riverine Material From Multiple Rivers in the Chesapeake Bay: Important Control of Estuarine Circulation on the Material Distribution

Jiabi Du
Virginia Institute of Marine Science, jiabi@vims.edu

Jian Shen
Virginia Institute of Marine Science, shen@vims.edu

AGU PUBLICATIONS

JGR

Journal of Geophysical Research: Biogeosciences

RESEARCH ARTICLE
10.1002/2016JG003707

Key Points:
- Estuarine circulation strongly affects the vertical and horizontal distributions of riverine material in the mainstem
- Material from tributaries has high potential to be transported to the upper estuary, despite its low concentration in the mainstem
- This study reveals three distinct spatial patterns in the mainstem of an estuary for materials from various sources

Supporting Information:
- Supporting Information S1

Correspondence to:
J. Du,
jiabi@vims.edu;
jiabi.du@gmail.com

Citation:
Du, J., & Shen, J. (2017). Transport of riverine material from multiple rivers in the Chesapeake Bay: Important control of estuarine circulation on the material distribution. *Journal of Geophysical Research: Biogeosciences*, *122*, 2998–3013. https://doi.org/10.1002/2016JG003707

Received 7 NOV 2016
Accepted 24 OCT 2017
Accepted article online 30 OCT 2017
Published online 18 NOV 2017

Transport of Riverine Material From Multiple Rivers in the Chesapeake Bay: Important Control of Estuarine Circulation on the Material Distribution

Jiabi Du[1] **and Jian Shen**[1]

[1]College of William and Mary, Virginia Institute of Marine Science, Gloucester Point, VA, USA

Abstract Driven by estuarine circulation, material released from lower Chesapeake Bay tributaries has the potential to be transported to the upper Bay. How far and what fraction of the material from tributaries can be carried to the upper estuary have not been quantitatively investigated. For an estuary system with multiple tributaries, the relative contribution from each tributary can provide valuable information for source assessment and fate prediction for riverine materials and passive moving organisms. We conducted long-term numerical simulations using multiple passive tracers that are independently released in the headwater of five main rivers (i.e., Susquehanna, Potomac, Rappahannock, York, and James Rivers) and calculated the relative contribution of each river to the total material in the mainstem. The results show that discharge from Susquehanna River exerts the dominant control on the riverine material throughout the entire mainstem. Despite the smaller contribution from the lower-middle Bay tributaries to the total materials in the mainstem, materials released from these rivers have a high potential to be transported to the middle-upper Bay through the bottom inflow by the persistent estuarine circulation. The fraction of the tributary material transported to the upper Bay depends on the location of the tributary. Materials released near the mouth are subject to a rapid flushing process, small retention time, and strong shelf current. Our results reveal three distinct spatial patterns for materials released from the main river, tributary, and coastal oceans. This study highlights the important control of estuarine circulation over horizontal and vertical distributions of materials in the mainstem.

1. Introduction

Chesapeake Bay, the largest estuary in the United States, has a well-defined mainstem that connects numerous tributaries. Five major rivers (i.e., Susquehanna River, Potomac River, Rappahannock River, York River, and James River) contribute about 90% of the total freshwater discharge to the Chesapeake Bay (Guo & Valle-Levinson, 2007; Hargis, 1980). The Susquehanna River, located at the north end of the Bay, is widely known to exert a dominant control on a variety of aspects in the middle-upper Bay, significantly affecting the stratification, sedimentation, nutrient levels, dissolved oxygen, and contaminants in this region (Ko & Baker, 2004; Schubel & Pritchard, 1986; Shen et al., 2012). Meanwhile, materials discharged from the main tributaries (e.g., Potomac, Rappahannock, York, and James Rivers) have the potential to be transported to the middle-upper Bay through the bottom layers by the persistent gravitational circulation (Goodrich & Blumberg, 1991). How far, and what fraction of, the material discharged from these tributaries can be transported toward the upper estuary has not been well investigated quantitatively. It is of interest to know the relative contributions of the material discharged from different tributaries to the material at different locations in the mainstem, which will provide valuable information for water quality management, source assessment, and prediction of the fate of substances, such as pollutants, nutrients, harmful algae seeds, and passive floating fish larvae.

The persistent gravitational circulation in the Chesapeake Bay has been well studied, and it is generally believed to have great impact on the water exchange between the mainstem and tributary and between the Bay and the coastal ocean (Austin, 2002; Du & Shen, 2016; Shen & Wang, 2007; Valle-Levinson, Wong, & Bosley, 2001). The net movement of bottom water between tributaries and the Bay's mainstem greatly affects the extent and duration of hypoxia in the tributaries (Kuo & Neilson, 1987). Due to the persistent gravitational circulation, the difference of residence time between the bottom and the surface in the mainstem can be as large as 100 days (Du & Shen, 2016). The Chesapeake Bay Program conducted a conservative

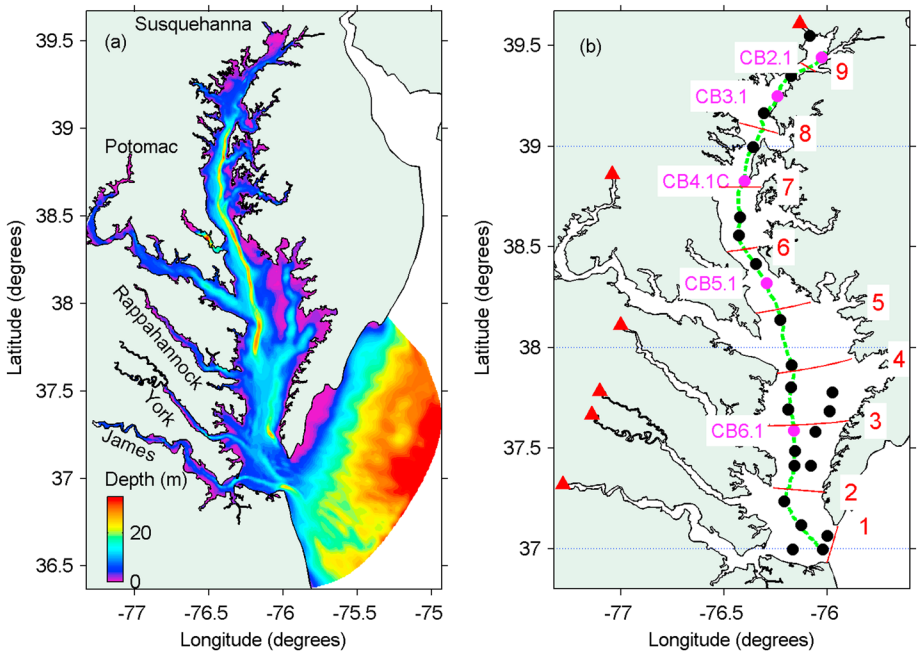

Figure 1. (a) Bathymetry of Chesapeake Bay, showing names and locations of five main rivers. (b) Nine cross sections in the mainstem are represented by red lines, with section numbers shown in red text; the longitudinal section along the deep channel is marked with a dash green line; red solid triangles denote the tracer releasing location; mainstem monitoring stations are marked with black or pink solid circle; the separations between lower Bay, middle Bay, and upper Bay are signified by dotted blue lines.

tracer simulation for the year of 1987 and found that the tributaries in the lower Bay had limited contribution to the upper Bay (Butt et al., 2000). The limited contribution from the lower Bay tributaries is largely due to its small discharge and cannot be interpreted as the low possibility of the material discharged from the tributaries being transported to the upper Bay. Large variability and high concentration of trace metals in local regions (e.g., Baltimore Bay and Hampton Roads) have been observed (Sinex & Wright, 1988; Skrabal, 1995). However, it is not well known how these local sources will affect the concentration in the mainstem spatially. Therefore, a quantitative study of the influence of estuarine circulation on the transport of materials discharged from tributaries, especially the lower Bay tributaries, is needed.

The present study is intended to investigate the transport of dissolvable riverine material and the relative contribution from five main rivers through a numerical modeling approach by conducting a long-term simulation of transport of multiple passive tracers independently released at the headwaters of five main rivers (i.e., Susquehanna, Potomac, Rappahannock, York, and James Rivers). Total nitrogen is chosen as an example of the riverine materials. The control of physical transport on the redistribution of total nitrogen is investigated based on the numerical modeling result and the long-term observation data collected from Chesapeake Bay Program (http://www.chesapeakebay.net). The article is organized as follows. The numerical simulations and the method to compute the tracer influx and outflux are described in section 2. The spatial distribution of tracer concentration, the relative contribution from different rivers, and the results of total nitrogen simulation are presented in section 3. The importance of gravitational circulation on the vertical and horizontal distributions of riverine material will be discussed in section 4, followed by a summary in section 5.

2. Methods

2.1. Numerical Model

We used the Environmental Fluid Dynamics Code (EFDC) (Hamrick, 1992) to simulate the hydrodynamics of the Chesapeake Bay from 1984 to 2014. EFDC uses a boundary-fitted curvilinear grid in the horizontal and sigma grids in the vertical. The model configuration and boundary condition are the same as those employed in Hong and Shen (2012) and Du et al. (2017). The bathymetry is shown in Figure 1a. A grid with a horizontal

cell matrix with dimensions of 112 × 240 and 20 evenly spaced sigma layers in the vertical was utilized. The model was forced by observed tide interpolated from three monitoring stations (i.e., 08651370 Duck, NC; 08638863 CBBT, VA; and 08557380 Lewes, DE) at the open boundary (http://tidesandcurrents.noaa.gov), freshwater discharges of main rivers (http://waterdata.usgs.gov/nwis/), and wind obtained from the North America Regional Reanalysis (NARR) produced at the National Center for Environmental Prediction (http://www.esrl.noaa.gov/psd/thredds/catalog/Datasets/NARR/pressure/catalog.html).

This model has been calibrated for surface elevation, current, and salinity for the Chesapeake Bay, and it simulated reliable stratification and destratification responses temporally and spatially in both wet and dry years (Hong & Shen, 2012, 2013; Shen et al., 2013).

2.2. Tracer Release Simulations

A passive tracer was independently and continuously released at the headwater of each of the five rivers, with a constant concentration of 1.0 (arbitrary unit) for all layers. The tracer concentration at the headwaters is evenly distributed in the vertical. Releasing the tracer at the headwater also has the advantage of using concentration rather than tracer mass, which is more convenient to implement. For all the tracer release simulations, the tracer concentration at the open boundary is set to zero. As the constant concentration of 1 (arbitrary unit) is used for all tracer release simulations, the tracer concentration at any location shows the distribution corresponding to the tracer discharged at its discharge location. Therefore, it can serve as a useful index to estimate the dilution strength and to predict the concentration of the corresponding material if given the concentration at the release location.

To examine the relative importance of the bottom influx and surface outflux in the transport of riverine material within the mainstem, we computed transverse and vertical integrals of the tracer influx and tracer outflux for nine selected cross sections in the mainstem (section locations are shown in Figure 1b). The influx and outflux were calculated using the long-term mean tracer concentration and residual along-channel velocity.

$$F_{\text{in}} = \int_{-H}^{0}\int_{\text{west}}^{\text{east}} VC\,dz\,dx, \text{ with } V = 0, \text{if } V < 0 \tag{1}$$

$$F_{\text{out}} = \int_{-H}^{0}\int_{\text{west}}^{\text{east}} VC\,dz\,dx, \text{ with } V = 0, \text{if } V > 0 \tag{2}$$

where V is the along-channel residual velocity (positive to the upper estuary and negative to the lower estuary) and C is the tracer concentration, both of which are averaged over the past three decades. H is the water depth. The water flux is calculated by setting the value of C to 1.0. Table 1 lists the long-term mean water influx at each cross section, which shows a rather large water influx in the lower and middle Bay. The magnitude of the water influx in the lower Bay is 3000–5000 $m^3\ s^{-1}$, which is of the same order from the measurements at the Bay mouth (Wong & Valle-Levinson, 2002). The magnitude of the water influx in lower-middle Bay is about twice the total mean river discharge (~2200 $m^3\ s^{-1}$ for the entire Bay), suggesting a high potential for material near the bottom to be transported toward the upper estuary. The water influx decreases from section 3 to section 9, and there is no water influx at the northernmost section.

Table 1
The Water Influx at Nine Cross Sections; the Cross-Section Location Is Shown in Figure 1b; Influx Values Were Calculated Based On the Residual Velocity Field, Which Is the Average of the Velocity Over the Past Three Decades

Section no.	Influx (m^3/s)
1	4,266.44
2	3,705.25
3	4,957.67
4	4,444.21
5	3,381.00
6	2,208.88
7	2,475.94
8	1,647.79
9	0.00

The relative contribution at a given location is measured by the tracer fraction P_i, which is the ratio of tracer mass discharged from a given river to the total mass discharged from all five rivers.

$$P_i = \frac{C_i}{\sum_{j=1}^{5} C_j} \tag{3}$$

where C_i is the concentration of tracer released from river i. The fraction can serve as an index to estimate the relative probability of the material discharged from different rivers.

Because of the large bottom inflow, the coastal ocean source can also be an important source of the material in the estuary. It has been well known that the coastal ocean provides large amount of phosphates to the estuary (Boynton et al., 1995; Nixon et al., 1996). The harmful

algae bloom seeds are abundant in the coastal sea, which can be transported into the estuary through the bottom inflow and serves as an important source for the local harmful algae bloom (Anderson et al., 2005, 2008; Marshall et al., 2005). Understanding the transport of the coastal ocean input is of interest. To examine the distribution of the material from coastal ocean input, a simulation for material input from the coastal ocean was also conducted. The release location for the coastal ocean input is the same as the offshore open boundary. The tracer concentration at the open boundary is set to 1.0 (arbitrary unit) for each layer.

2.3. Simulating the Total Nitrogen

The eutrophication model has been applied to simulate nitrogen dynamics in estuaries (e.g., Cerco & Cole, 1993; Park et al., 1995). For these models, nitrogen state variables include particulate organic nitrogen (PON), dissolved organic nitrogen (DON), ammonium (NH_4), nitrate, and nitrite (NO_{23}). The general model can be described as

$$\frac{\partial \mathrm{PON}}{\partial t} + T(\mathrm{PON}) = L_{\mathrm{PON}} + R_{\mathrm{PON}} - k_{\mathrm{DON}}\mathrm{PON} - w_{\mathrm{PON}}\mathrm{PON} \tag{4}$$

$$\frac{\partial \mathrm{DON}}{\partial t} + T(\mathrm{DON}) = L_{\mathrm{DON}} + R_{\mathrm{DON}} + k_{\mathrm{DON}}\mathrm{PON} - k_{\mathrm{NH4}}\mathrm{DON} \tag{5}$$

$$\frac{\partial \mathrm{NH4}}{\partial t} + T(\mathrm{NH4}) = L_{\mathrm{NH4}} + k_{\mathrm{NH4}}\mathrm{DON} + F_{\mathrm{NH4}} + R_{\mathrm{NH4}} - k_{\mathrm{NO3}}\mathrm{NH4} - \mathrm{UP}_1(\mathrm{Chla}) \tag{6}$$

$$\frac{\partial \mathrm{NO23}}{\partial t} + T(\mathrm{NO23}) = L_{\mathrm{NO23}} + k_{\mathrm{NO3}}\mathrm{NH4} + F_{\mathrm{NO23}} - \mathrm{UP}_2(\mathrm{Chla}) - k_{dni}\mathrm{NO3} \tag{7}$$

$$\frac{\partial \mathrm{Chla}}{\partial t} + T(\mathrm{Chla}) = (g - r - m)\mathrm{Chla} + L_{\mathrm{Chla}} - w_{\mathrm{chla}}\mathrm{Chla} \tag{8}$$

where L_x denotes external loading (x = PON, DON, NH_4, NO_{23}, and Chla), k_x denotes reactions, F_x denotes bottom flux, and w_{PON} and w_{Chla} denote settling. UP_1 and UP_2 are nutrient uptakes by phytoplankton. Rx denotes nutrient recycle. g, r, and m are phytoplankton growth, respiration, and mortality rates. The growth rate is a function of light, nutrient, and temperature. T denotes transport and dispersion processes.

By summing equations (4)–(8), total nitrogen (TN) can be expressed as

$$\frac{\partial \mathrm{TN}}{\partial t} + T(\mathrm{TN}) = L\mathrm{sum} - (w_{\mathrm{PON}}\mathrm{PON} + k_{din}\mathrm{NO3} + \alpha w_{\mathrm{chla}}\mathrm{Chla} - F_{\mathrm{NH4}} - F_{\mathrm{NO23}}) - [\mathrm{UP}_1(\mathrm{Chla}) + \mathrm{UP}_2(\mathrm{Chla}) - R_{\mathrm{PON}} - R_{\mathrm{DON}} - R_{\mathrm{NH4}}] \tag{9}$$

where α is N : Chla ratio. The term Lsum is the total external nitrogen loading. The sum of other terms can be regarded as total net removal of TN. If assuming that the total removal is proportional to TN, TN transport can be simplified as

$$\frac{\partial \mathrm{TN}}{\partial t} + T(\mathrm{TN}) = L\mathrm{sum} - k_{\mathrm{TN}}\mathrm{TN} \tag{10}$$

TN can be therefore simulated with a prescribed loading and a removal rate. Previous studies show that annual TN removal rate in different estuaries does not change dramatically (Dettmann, 2001; Nixon et al., 1996). Based on Boynton et al. (1995) and Dettmann (2001), the average annual removal rate for TN for the Chesapeake Bay is about 0.06 day^{-1}. The removal of TN is mainly caused by burial processes, denitrification, and transport out of the estuary (Boynton et al., 1995).

The TN loading below the fall-line at the major rivers is based on the U.S. Geological Survey (USGS) observations (https://cbrim.er.usgs.gov), and the point source and atmosphere deposition are estimated based on their ratios suggested by Boynton et al. (1995). Based on recent nutrient loading monitoring and estimations by the USGS and the Chesapeake Bay Program, the decadal mean of total nitrogen loading, L, is about 150×10^6 kg/yr, of which about 90×10^6 kg/yr (~60%) is from the nonpoint source input and 40% is from atmospheric deposition and point sources (https://cbrim.er.usgs.gov/). The diffusive loading is added directly at the headwater of major rivers, while the point source loading and atmospheric loading are added along the banks of the mainstem. Additionally, we used a constant TN concentration of 0.15 mg/L as long-term mean at the open boundary (Levitus et al., 1993; Voss et al., 2013). For simplicity, this TN concentration is prescribed to the model grids of the coastal ocean boundary. The open boundary condition could have a great impact on the TN concentration, especially in the lower Bay and the Bay mouth area. This approach can be

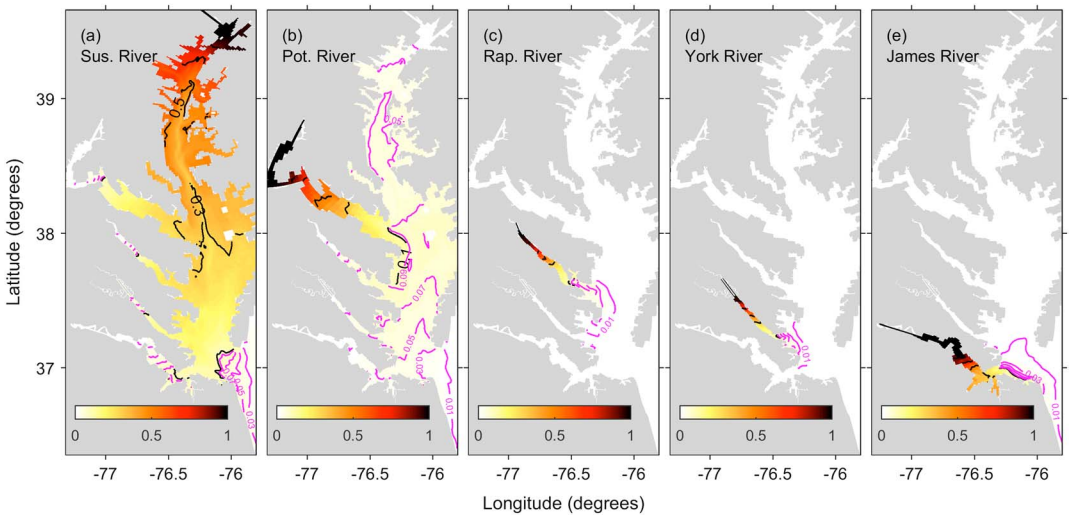

Figure 2. Distribution of vertical mean tracer concentration for each river release; two groups of contour lines are used; a solid black line with a 0.2 interval is used for values 0.1–0.9 and a pink line with a 0.02 interval is used for values 0.01–0.09.

considered as the first order approximation, which enables us to conduct a model study to understand the influence of the physical transport processes on TN distribution in the Bay.

Simulation of the TN is conducted for 1985–2012, and the simulation results are compared with the observation data collected from the Chesapeake Bay Program. We analyzed the long-term mean condition and the monthly and interannual variations of the TN in the mainstem.

3. Result

3.1. Horizontal Distribution of the Tracer Concentration

For all the tracer release simulations, tracer concentrations decrease down-estuary because of quick dilution by large volumes of water in the mainstem (Figure 2). Depending on the magnitude of discharge and the relative location of the river mouth to the mainstem, the tracer concentration varies significantly for different rivers. Here we use a tracer concentration of 1% as a criterion to determine if the river input has influence for a given region.

Not surprisingly, discharge from the main river, Susquehanna River, has the most significant influence in the mainstem, which is due to its largest river discharge and its most upper estuary location (i.e., at the head of the Bay). The tracer concentration from Susquehanna input is about 50%, 30%, and 10% at latitudes 39 N, 38 N, and 37 N in the mainstem, respectively (Figure 2a). Its influence is also evident in the lower reach, even the middle reach, of other subestuaries.

The Potomac River has the second largest influence area, despite the relatively smaller tracer concentration ($<$10%) in the mainstem in comparison with the Susquehanna River release. The tracer concentration decreases quickly from 100% at the river head to 10% at the river mouth (Figure 2b). In the Bay's mainstem, its concentration decreases toward both the upper Bay and the lower Bay.

For the other three tributaries, i.e., Rappahannock, York, and James Rivers, the tracer concentration exhibits a similar pattern, with a rather small influence area in the mainstem due to the small river discharge and/or a quick dilution by the large volume of water in the lower Bay. Particularly, tracer from the James River, which has river discharge of the same magnitude as the Potomac River, highly concentrated near the western bank. The tracer concentration at the mouth of any of the three rivers is around 3% (Figures 2c–2e). The outreach of the 1% isoline is very limited, suggesting that riverine material from these rivers is quickly diluted.

3.2. Vertical Distribution Along the Mainstem

The vertical difference of tracer concentration along the deep channel section of the Bay's mainstem is evident, with a larger concentration near the surface from the river mouth down to the Bay's mouth and a

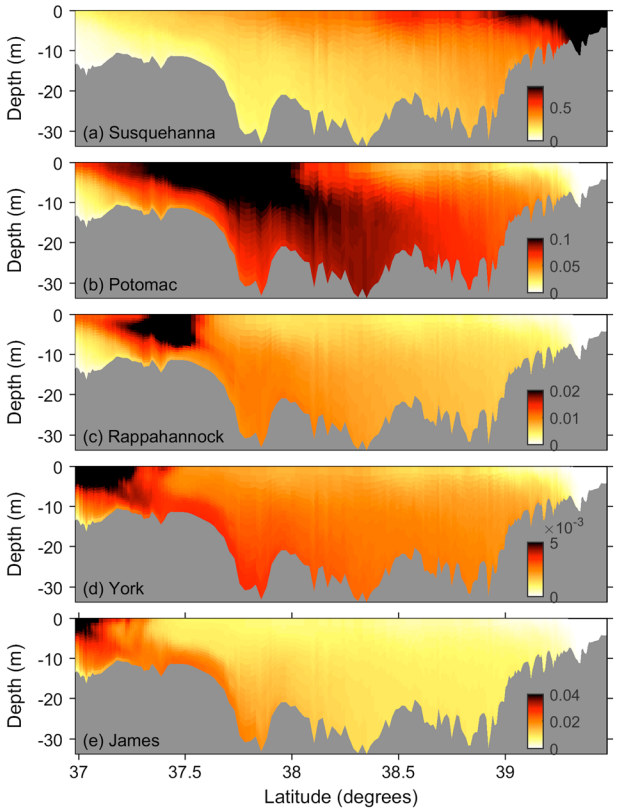

Figure 3. The vertical profile of tracer concentration along the longitudinal section for tracers released from (a) Susquehanna River, (b) Potomac River, (c) Rappahannock River, (d) York River, and (e) James River. The color scale is different for different rivers.

larger concentration near the bottom from the river mouth up to the upper Bay (Figures 3 and S1 in the supporting information). For the Susquehanna River release, the larger surface tracer concentration is observed over the entire Bay's mainstem, which can be attributed to the buoyancy force induced by the large freshwater discharge. The vertical difference of the tracer concentration released from any other tributary exhibits an obviously different pattern, compared to that of the main river release. Taking Potomac River as an example, the tracer concentration decreases toward both the upper Bay and the lower Bay, with a larger concentration in the bottom layers in the upper Bay and a smaller concentration in the bottom layers in the lower Bay (Figure 3b). For discharge from other tributaries (i.e., Rappahannock, York, and James), the tracer concentration exhibits a similar vertical pattern as with the Potomac River (Figures 3b–3e). Materials from the lower Bay tributaries cannot reach to the north end of the mainstem, because there is no bottom inflow at the north end of the mainstem (Table 1).

3.3. Lateral Distribution Across the Mainstem

The vertical difference of tracer concentration is obvious not only along the deep channel in the mainstem but also across the mainstem. The asymmetry of the tracer concentration between the Bay's Eastern Shore and Western Shore occurs in almost all cross sections (Figure 4). Sections 1–3 in the lower Bay and section 6 in the middle-upper Bay are selected to examine the lateral distribution of tracer concentration. Much lower concentration in the Eastern Shore is observed at the section near the tributary mouth (e.g., sections 2 and 3 for York and Rappahannock Rivers input, respectively), where material tends to move along the Western Shore by the strong seaward residual current (Figure 5). The tracer concentration isolines show moderate to strong tilting across the mainstem (Figure 4). The tilting of isolines is related to the horizontal shear of the exchange flow (Figure 5), and the tilting strength is related to the width of the channel (Valle-Levinson, Reyes, & Sanay, 2003). A strong tilting of both the tracer concentration and the residual current is found in section 3 (Figures 4c and 5c), which has the largest width among the four selected sections. From the tributary mouth to the Bay mouth, the tracer concentration is greater at surface layers and along the Western Shore, which is evident in section 1 (located at the mouth). On the contrary, from the tributary mouth to the upper Bay, the tracer concentration is larger along the Eastern Shore and larger in the bottom layers. In addition, the vertical difference in sections 2–6 is much smaller than that in section 1. Tracer concentration at the surface ranges from 30 to 43 times that at the bottom in section 1, while there is less difference between the bottom and the surface in sections 2–6. The larger vertical difference near the Bay's mouth is believed to be related with the shorter residence time and southward shelf current outside the mouth, which will be further discussed in section 4.2.

3.4. The Tracer Influx and Outflux

The product of the water flux and the tracer concentration is calculated as tracer flux (equations (1) and (2)) to understand the relative magnitude of tracer influx and outflux. The tracer influx and outflux normalized by the river discharge are shown in Figure 6. The ratio of the tracer influx to the river discharge can be as large as 119% (Figure 6b), suggesting that a large portion of material in the lower estuary can be transported to the upper estuary. Note that the 119% ratio cannot be interpreted as a net transport of 119% of the material toward the upper estuary, as the net transport is the sum of influx and outflux. For any release, all the material will be ultimately exported out of the Bay. Influenced by the magnitude of river discharge and the location of the river's mouth, the tracer influx and outflux ratios in the mainstem vary dramatically, with a maximum influx ratio ranging from 18% (at section 3 for the York River release) to 119% (at section 4 for the Potomac River release).

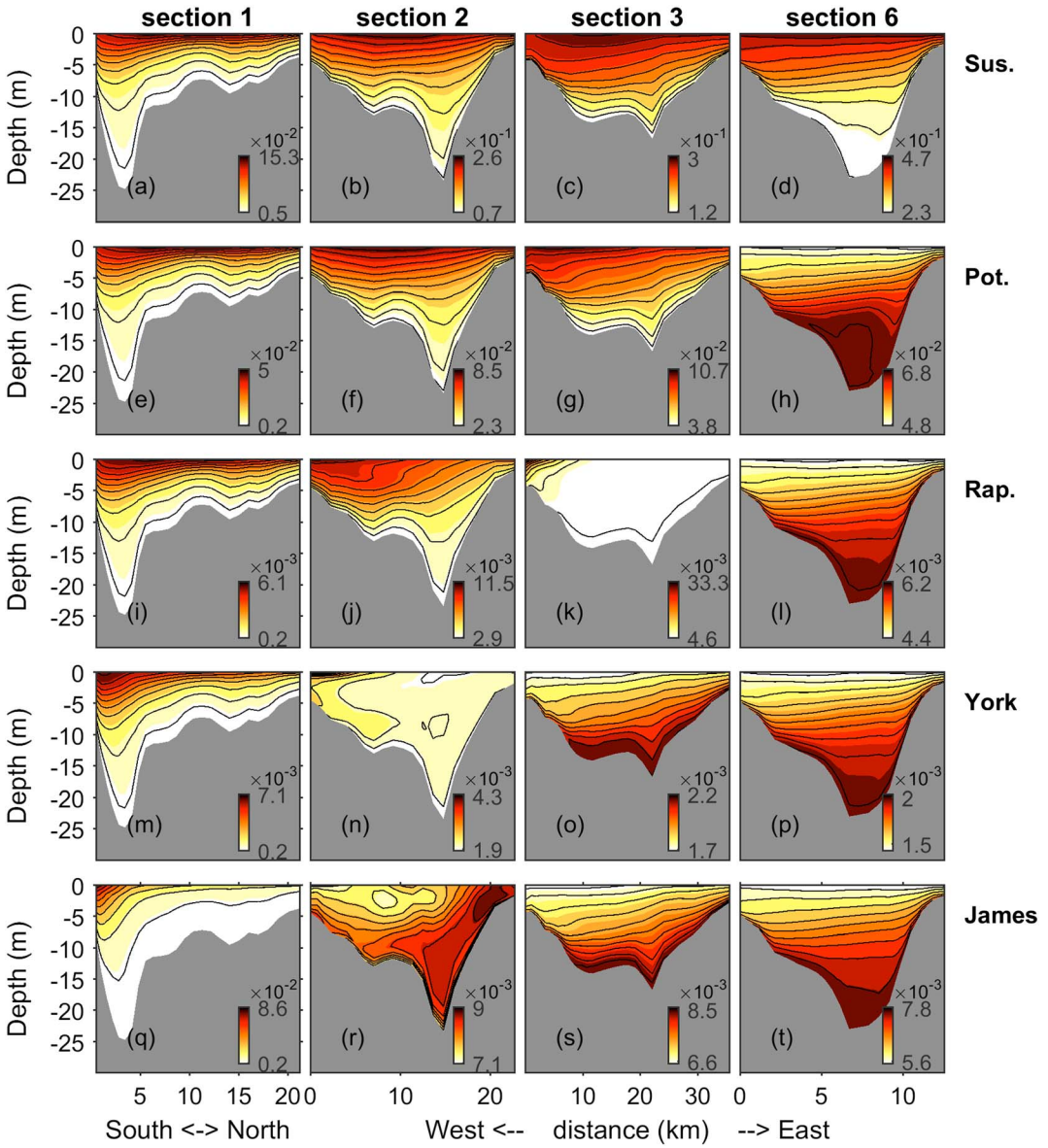

Figure 4. The vertical profiles of tracer concentration at sections 1–3 and 6 for tracer released from (a–d) Susquehanna River, (e–h) Potomac River, (i–l) Rappahannock River, (m–p) York River, and (q–t) James River. The maximum and minimum values for each section are shown along the color scale.

The maximum tracer influx ratio usually occurs in the lower Bay, at either section 3 or section 4, and the tracer influx decreases toward both upper Bay and lower Bay. Sections 3 and 4 have the largest influx among all the sections, probably due to the large widths of these two sections. Among all the five rivers, the Potomac River has the largest maximum tracer influx ratio with a value of 119%, followed by 98% and 94%, respectively, for the Susquehanna and Rappahannock Rivers. Surprisingly, the tracer influx ratio for the Rappahannock River is rather large (maximum 94%), despite its small tracer concentration in the mainstem (less than 3%, Figure 2c). In the middle-upper Bay, the mean tracer influx ratio value is largest for Susquehanna, followed by Potomac, Rappahannock, York, and James. Taking section 8 as an example, the tracer influx ratio from the Potomac River release is 7 times larger than that from the James River release. James River and York River have the smallest mass influx ratios at almost all cross sections, except section 1. Even though other smaller tributaries are not included in the simulations, it is confident to predict that material released at tributaries in the middle and upper Bay is very likely to have a large tracer influx.

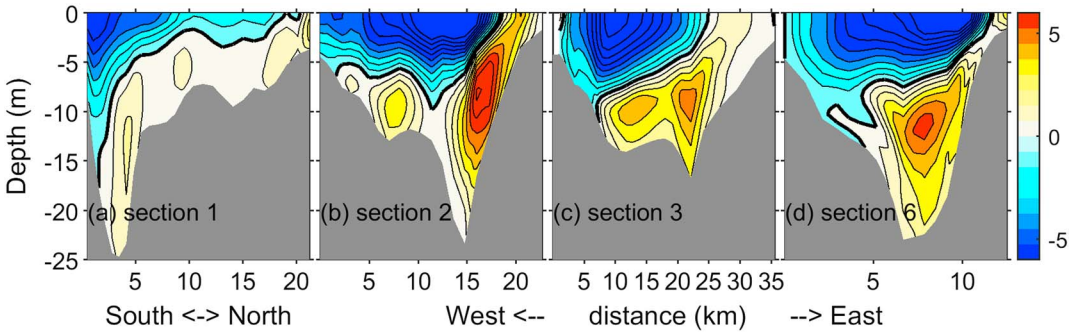

Figure 5. Residual along-channel velocity (cm/s) for (a) Section 1, (b) Section 2, (c) Section 3, and (d) Section 6. Positive values represent influx moving up-estuary. The isoline for value zero is marked with a bold black line. The interval between adjacent isolines is 1 cm/s.

3.5. Relative Contribution From Each River

The relative contribution (equation (3)) indicated by the fraction of discharged material from each river to the total materials discharged from five rivers varies dramatically among different river releases. The results provide a measure of the contribution of each tributary assuming that the concentration of material discharged from each river is the same. The Susquehanna River source dominates over the entire mainstem, with the tracer fraction ranging from 50% at the Bay's mouth to 100% at the Bay's head (Figures 7a and S2). Material from the Susquehanna River also has a large contribution in the lower reaches, even in the middle reaches, of subestuaries in the lower-middle Bay. The tracer fraction from the Potomac River input is less than the Susquehanna River input but much larger than the inputs from the Rappahannock, York, and James Rivers (Figures 7b–7e). The mean contributions averaged over the mainstem are about 70%, 20%, 3%, 2%, and 5% for the Susquehanna, Potomac, Rappahannock, York, and James Rivers, respectively (Figure S3).

Different from the dominant contributions of the Susquehanna and Potomac, the contributions from the Rappahannock, York, and James are very limited in the Bay's mainstem. Among these three tributaries, York River has the least contribution to the mainstem. For the York River, the 1% isoline cannot even reach to the middle Bay. James River, on the other hand, has a larger influence, with its 1% isoline extending to

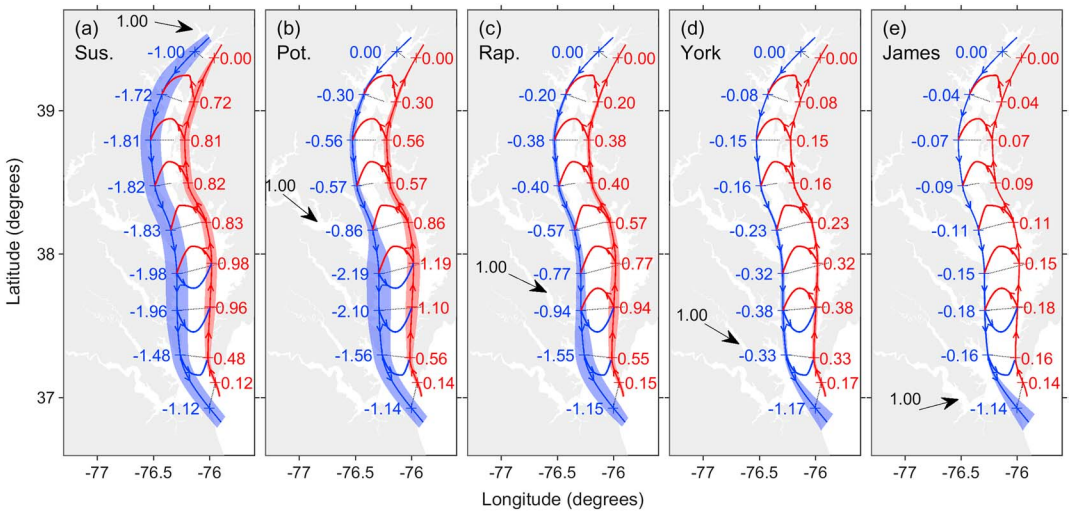

Figure 6. Pathway of riverine material from (a) Susquehanna River, (b) Potomac River, (c) Rappahannock River, (d) York River, and (e) James River. The blue lines on the left show the tracer outflux to the lower Bay, and the red lines on the right show the tracer influx to the upper Bay. Nine cross sections in the mainstem are shown with dotted lines, and the influx and outflux ratios relative to the net river loading are shown in text. A larger shadow denotes a larger flux. The arrow between the bottom tracer influx and surface tracer outflux denotes the net vertical flux, with red arrows denoting a net upward tracer flux and blue arrows denoting a net downward tracer flux.

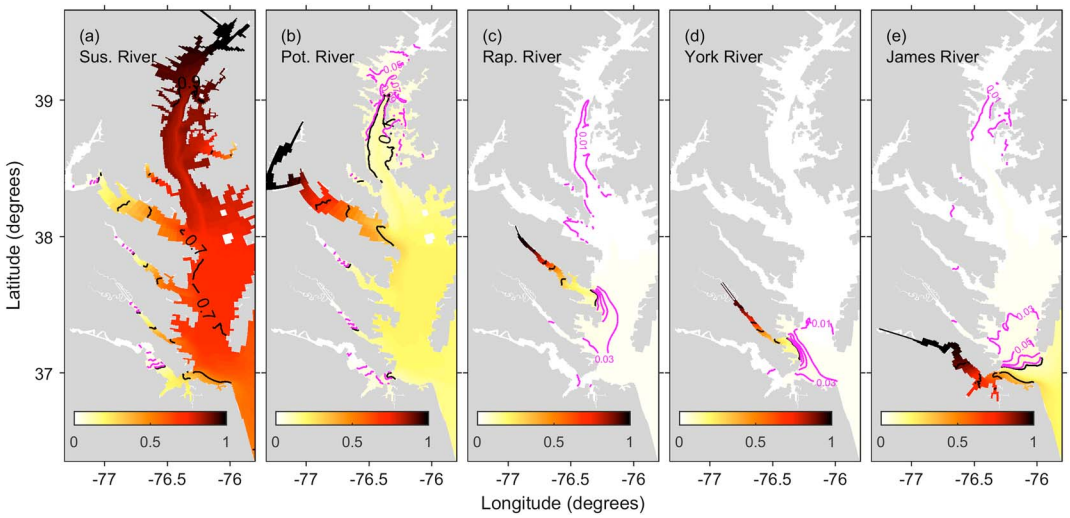

Figure 7. The distribution of the relative contribution for five main rivers, assuming the same material concentration at headwater of all the rivers; two groups of contour lines are used, a solid black line with a 0.2 interval for values 0.1–0.9 and a pink line with a 0.02 interval for values 0.01–0.09.

as far as the upper Bay (Figure 7e). James River has a large contribution (20–30%) in the shelf area near the Bay's mouth. Overall, the Susquehanna River input dominates the majority of the Bay, while inputs from tributaries dominate locally.

3.6. Material From the Coastal Ocean

A simulation of tracer release at the open boundary was conducted, and it reveals the high potential of coastal ocean material to be transported to the Bay and the subestuaries (Figure 8). Transport of material from the coastal ocean is highly similar to the process of salt intrusion. The incoming water mass from the coastal ocean is transported up-estuary mainly through the bottom inflow and affects the shoaling area and surface layer through vertical mixing and lateral transport, resulting in a larger concentration near the bottom and a lower concentration near the surface (Figure 8). The tracer concentration decreases toward the upper estuary, with a value of about 90% at the mouth, 60% at 38 N, and 40% at 39 N, respectively.

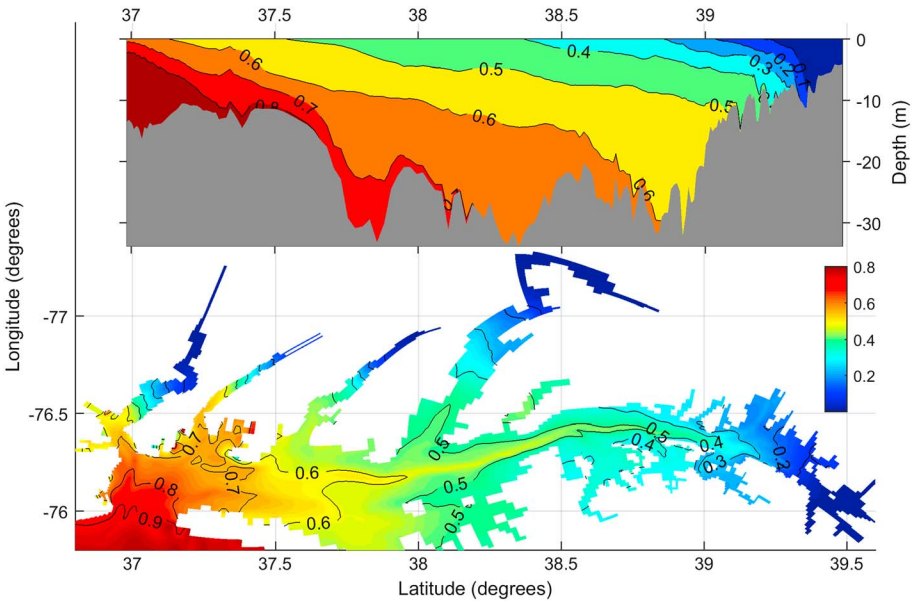

Figure 8. (top) Vertical profile of the tracer concentration along the longitudinal section and (bottom) the vertical mean tracer concentration from the coastal ocean input with an original concentration of 1.0 at the offshore boundary.

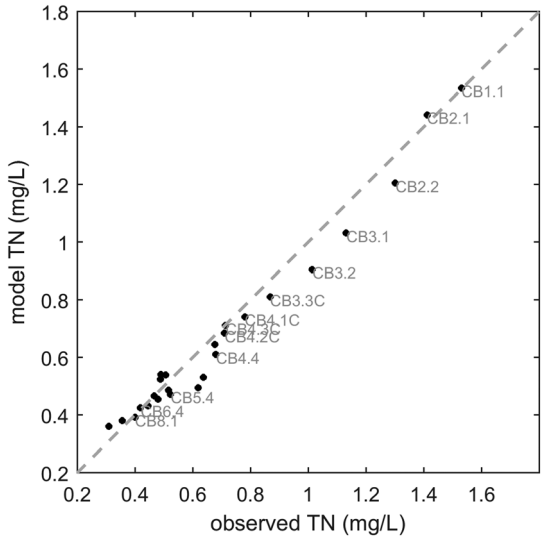

Figure 9. Scatterplot between the observed TN and modeled TN, with names of selected stations in gray text. The TN concentration is averaged for the entire water column and over the period of 1985–2012, representing the long-term mean.

3.7. Simulating the Total Nitrogen Redistribution

Despite the simplicity of the approach, the spatial distribution of the column mean TN averaged over 1985–2012 in the Bay's mainstem is well reproduced (Figure 9), suggesting a dominant control of the physical transport and location of riverine TN sources on the distribution of long-term mean value of TN. The results suggest that the mean removal rate of TN is 0.06 day^{-1} for the simulation period, which is consistent to the estimation by previous studies (e.g., Dettmann, 2001).

The temporal variations of the observed TN at several selected stations agree well with model results (Figure 10). The physical transport and the TN loadings explain 30–50% of the monthly variation and 50–90% of the interannual variation of the observed TN. The less percentage explained by the model in the lower Bay compared to the middle and upper Bay can be attributed to the interannual variation of coastal ocean condition (Levitus et al., 1993) and spatially-temporally varying nitrogen loss rate in the mainstem.

Further analysis of the seasonal difference between modeled and observed TN suggests that there is a significant seasonal variation of the TN removal rate. The model underestimates the TN concentration during the winter and early spring (Figure 11), especially in the middle and upper Bay, suggesting that the realistic nitrogen removal rate during winter and early spring is less than 0.06 day^{-1}, the constant removal rate used in the model.

4. Discussion

4.1. Important Control of Estuarine Circulation on the Distribution of Riverine Material

The distribution of riverine material is greatly regulated by the persistent estuarine circulation. The estuarine circulation is generally believed to play a major role in the aggregation of sediment in the turbidity maximum zone (Festa & Hansen, 1978; Sanford, Suttles, & Halka, 2001), the larvae transport for a variety of species of fish

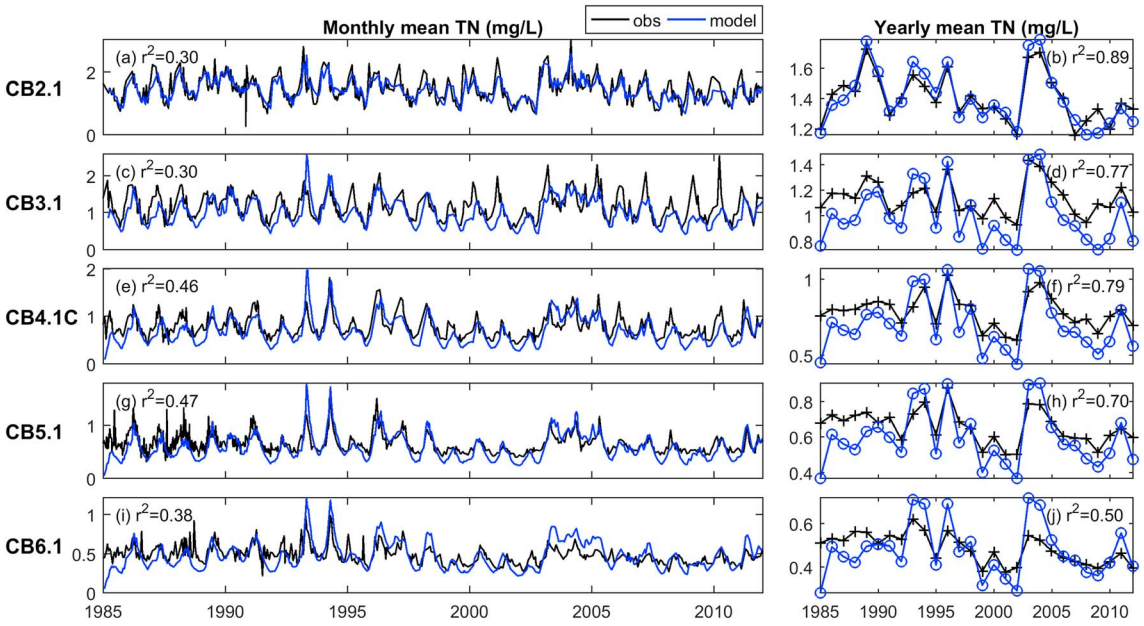

Figure 10. Time series of the observed TN and modeled TN at station CB2.1, CB3.1, CB4.1, CB5.1, and CB61, with (left column) monthly mean time series and (right column) annual mean time series. The coefficient r^2 of the linear regression between the modeled and observed values is shown on the top of each panel.

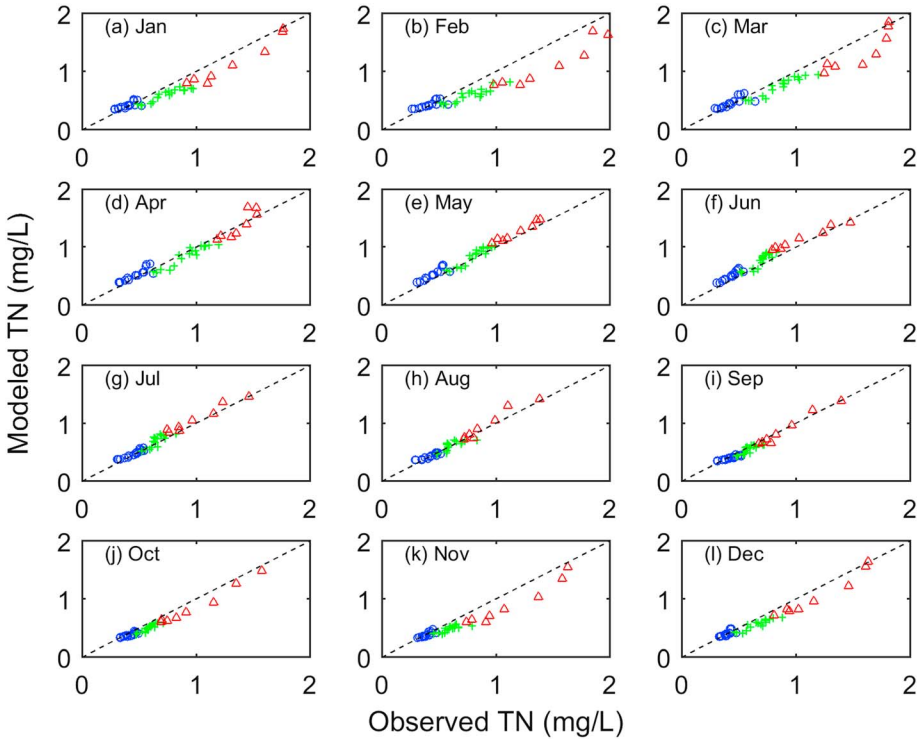

Figure 11. The scatterplot between modeled and observed TN values at 26 mainstem stations for each month averaged over 1985–2012. The location of the mainstem stations is shown with pink filled circles in Figure 1b. Stations in the upper Bay (CB1.1–CB3.3), middle Bay (CB4.1–CB5.5), and lower Bay (CB6.1–CB8.1) are denoted with red triangles, green crosses, and blue circles, respectively.

(Epifanio & Garvine, 2001; Fortier & Leggett, 1983), and the hypoxia condition (Du & Shen, 2015; Kemp et al., 2005; Kuo & Neilson, 1987).

The vertical distribution is mainly caused by the unique manner of water exchange between the estuary and adjacent coastal ocean and between tributary and mainstem. Material released from the Susquehanna River tends to concentrate near the surface, leading to a net downward transport through vertical mixing and lateral transport processes in the mainstem. Because of the bottom influx, the surface outflux can be as large as 190% of the river discharge (Figure 6a). This effect manifests in vertical differences in both the mainstem and the lower reach of other subestuaries, with a larger surface concentration in the mainstem and a smaller surface concentration in the subestuaries (Figure S1a). A large amount of material in the mainstem is transported into the tributaries in the bottom layers by gravitational circulation (Kuo & Neilson, 1987). This mechanism can be also applied to explain the vertical difference of material concentration from the input of other tributaries. Taking the material released from the Potomac River as an example, the bottom tracer concentration is larger in the upper Bay and the lower reaches of Rappahannock, York, and James Rivers (Figure S1b), because the most efficient way the material from the Potomac River is transported to these areas is through gravitational circulation.

Besides the along-channel distribution, the lateral distribution is also highly related to the estuarine circulation. The horizontal shear of exchange flow (Valle-Levinson et al., 2003) is a key factor controlling the lateral shape of tracer concentration. Even for a narrow channel, the horizontal shear of the exchange flow, induced by the Coriolis force, will cause a larger bottom inflow to the right of the channel (looking up-estuary from the estuary mouth). This lateral inequality of transport will lead to a lateral tilting of tracer concentration as shown in the vertical profiles of sections 2 and 3 (Figure 4). As the strength of tilting is related to the width of the cross section, a narrower cross section (e.g., section 6 in Figures 4 and 5) tends to have less horizontal shear of exchange flow and thus less tilting of tracer concentration isolines.

The channel topography can modulate the vertical mixing and stratification and thus affect the distribution of released material. The shallow topography in the lower Bay (37–37.5 N) contributes to the stronger vertical

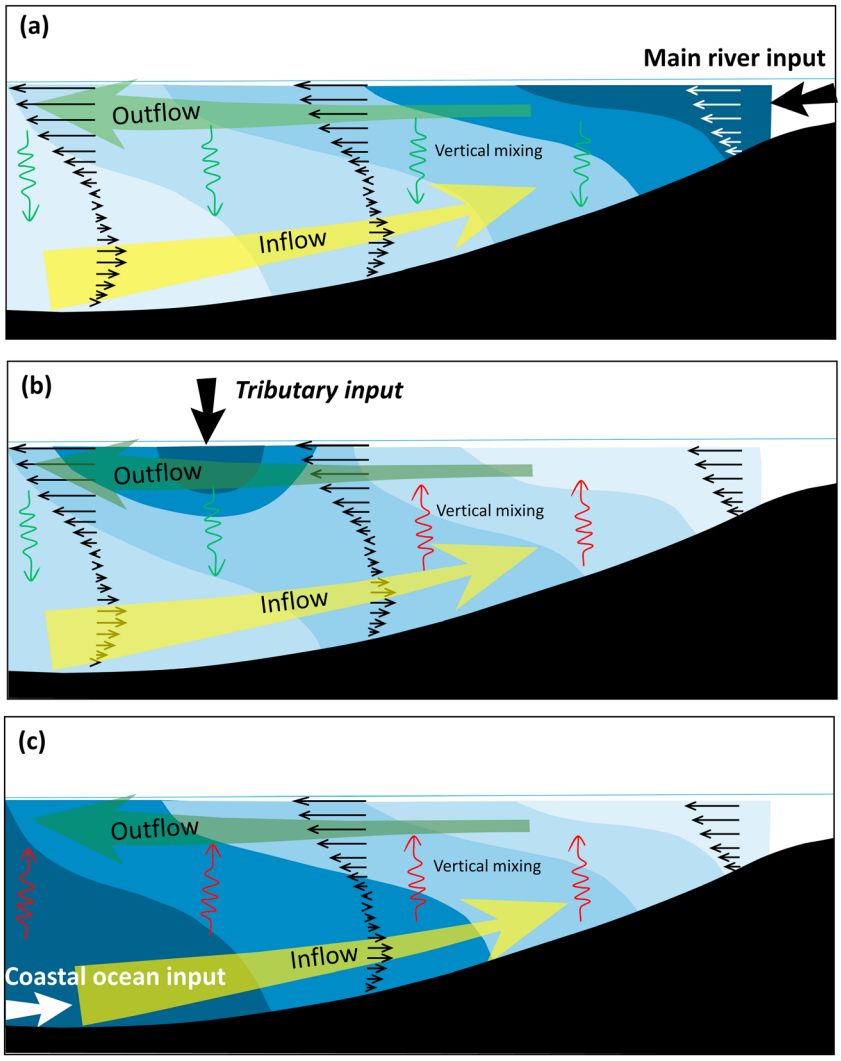

Figure 12. Conceptual diagrams to show the main processes affecting the transport of material from (a) main river input (e.g., Susquehanna River), (b) tributary input (e.g., Potomac, Rappahannock, York, and James Rivers), and (c) coastal ocean input. Filled color in gray scale denotes the material concentration. The magnitude of inflow in the bottom layers decreases toward the upper estuary, and the magnitude of the outflow increases toward the lower estuary. The residual circulation is shown by the black arrow, and there is no inflow at the upper end of the estuary. Different directions of the net vertical transport are marked with different colors.

mixing in this region. Without the contribution of the shallow topography in the region, the material released from the tributaries in the middle-upper Bay (e.g., Potomac River and Susquehanna River) is expected to be more concentrated at the surface layer.

4.2. Source Location Determines the Fraction of Material Moving Up-Estuary in an Estuary

The estuarine circulation, together with the source location, determines the spatial distribution of material from different sources. Figure 9 is a conceptual diagram illustrating the dominant processes that regulate the material distribution. The location of the source affects the material distribution, the magnitude of bottom tracer influx, and the relative contribution.

The source location greatly affects both horizontal and vertical distributions of the material. Substances discharged from the main river will spread to the lower estuary and concentrate in the surface layers (Figure 12a). The net vertically downward transport is mainly caused by both vertical mixing and lateral transport (Hong & Shen, 2013; Scully, 2010). A portion of the material near the bottom will be transported up-estuary by gravitational circulation. For tributary discharge, material concentrates near the mouth of

the tributary and is diluted in both landward and seaward directions. The net vertical transport direction is opposite between the lower estuary and upper estuary (Figure 12b). Material from the coastal ocean input will be transported into the upper estuary in the bottom layers by the persistent gravitational circulation, leading to an opposite spatial pattern as with the main river source (Figure 12c). The vertical net transport will be in the upward direction in the mainstem for the coastal ocean source.

The location of source highly affects the magnitude of the bottom tracer influx. The lower Bay is characterized by rapid flushing and small residence time (Du & Shen, 2016). The strong outflow near the southern shore at the mouth will export the material from the James and York Rivers quickly, and material exported usually has little chance to come back because of the southward river plume and southward shelf current (Guo & Valle-Levinson, 2007; Jiang & Xia, 2016; Lentz, 2008). The larger vertical difference near the mouth (where the surface concentration is 30–43 times that at the bottom) can also be attributed to the rapid flushing in this region. Tracers released at the upper estuary tend to have longer residence time inside the Bay. With a longer residence time, a larger fraction of material will be mixed down to the bottom layer through diffusion, vertical advection, and lateral and longitudinal circulation, leading to a smaller vertical difference. The quick flushing near the mouth also explains the much smaller tracer influx to the middle-upper Bay for the discharges from both York and James Rivers. It appears that the ratio of tracer influx to the river discharge will increase as the location of the mouth of the tributary moves up-estuary.

The different retention times for different sources also contribute to the inconsistency between the relative contribution of material in the mainstem and the relative river discharge. The contribution is not necessarily proportional to the discharge. For example, the relative contribution of Susquehanna is about 70%, which is larger than the percentage of its river discharge, which is about 60% of the total of the five river discharges. The contribution of input material from the James River is less than 5%, which is lower than its flow contribution (about 10%). The longer the residence time the material has inside the Bay, the larger the contribution will be.

Even though there is a high potential of material released from the tributaries in the lower Bay and the coastal ocean to be transported to the upper Bay, the movement toward the upper Bay in the bottom layers is very slow. The mean bottom inflow is with a magnitude of 1~2 cm/s, and thus, a water parcel at the mouth needs 100–200 days to reach the upper Bay (Hong & Shen, 2013; Shen et al., 2012). Transport of material released at the lower estuary is more sensitive to the coastal dynamics, such as upwelling, dispersion of the river plume, and shelf currents.

The tracer release experiments have been reported in several estuaries, and almost all experiments show that the material distribution is highly regulated by the physical processes, particularly by the flushing capacity and the residence time of the system. Tracers are also widely used to investigate the river plume (e.g., Hudson River (Hellweger et al., 2004)) and to scale the transport processes to quantify dispersion of living resources (e.g., James River (Guadiana Estuary, Oliveira, Fortunato, & Pinto, 2006; Shen et al., 1999)). Azevedo, Bordalo, and Duarte (2010) used a well-calibrated 3-D hydrodynamic model to simulate the contaminant dispersion by releasing tracers and found the important modulation of tide, river discharge, wind, and estuarine circulation on the redistribution of the contaminant. Caplow et al. (2003) studied the transport dynamics in the New York Harbor by injecting and measuring a chemical tracer, sulfur hexafluoride (SF6), and found that the low retention time of the estuary caused quick dilution and rather high loss rate, which is consistent with our tracer experiments for the material released in the lower Bay tributaries. Gustafsson and Bendtsen (2007) used age tracer to investigate the vertical mixing in a Fjord, where the signal of vertical mixing is not detectable in salinity and temperature fields. In our study, the tracer concentration along the deep channel section of Bay's mainstem reveals distinct vertical difference (Figures 3 and 4), which is otherwise not easy to detect without using tracers.

4.3. Limitations of the Passive Tracer Method

Even though the passive tracer method could serve as a useful tool to understand the redistribution of the soluble riverine materials, there are some limitations that should be pointed out as the passive tracer method omits some processes, such as the decay, settling, burial, and resuspension. Consequently, the relative contribution from the Susquehanna River on the TN in lower Bay may not be as large as shown in the result of passive tracer simulation because of the substantial loss during the transport that could take more than 100 days (Shen & Wang, 2007). By including the net removal rate of the TN, one can reasonably reproduce

the TN variation in the Bay. However, there are noticeable discrepancies between the modeled values and observed values, possibly due to the seasonal change of net removal rate. Several possible factors can contribute to the seasonal differences of the nitrogen loss rate, such as the seasonality of algal uptake, nitrification-denitrification, sediment resuspension, and dissolved nitrogen release from sediment (Baird, Ulanowicz, & Boynton, 1995; Cowan & Boynton, 1996; Kemp et al., 1990). The combination of these processes seems to result in an overall smaller nitrogen removal in the winter and early spring than in the summer and fall. In addition, the spatial variation of the net removal rate, which is related to the spatially varying biological and chemical environment, could introduce further discrepancy in the TN distribution. Therefore, to examine the detail variations for a specific substance subject to biogeochemical processes, it is always recommended to model explicitly including these biogeochemical reactions. For the TN in the Bay, using a net constant TN removal rate could well simulate the variation of TN, but for other nutrients or organic pollutant, adding a constant removal rate might not be sufficient. Nevertheless, the passive tracer simulation result retains the main characteristic of the redistribution pattern and could still provide important information for the potential pathway of riverine materials.

Several other factors are also important for the transport and the distribution of the nonconservative material, such as the solubility of the material, the settling velocity, the biogeochemical processes, and the duration and depth of the release. A different release depth could make a dramatic difference at different locations, which has been confirmed by multiple studies using particle tracking (e.g., North et al., 2008). The release time and the duration of release can make dramatic differences, especially for a large estuarine system as dynamics can change dramatically over a short period. Short-term events, such as storms, can alter the transport processes. The transport of material whose release lasts for only a short period is subject to short-term events, such as strong Ekman transport toward the coastal ocean, and a high-speed wind event that could well mix the entire water column and weaken the estuarine circulation (Cho et al., 2012; Li et al., 2006; Shen & Gong, 2009). Furthermore, materials with settling velocity will be subject to the bottom inflow in its earlier stage. Even though these specific properties of the material could modulate the spatial distribution, they are unlikely to shift the overall pattern of the distribution.

5. Conclusion

By using passive tracers, our numerical simulation highlights the important control of estuarine circulation on the redistribution of riverine material in a partially mixed estuary. Driven by the persistent bottom inflow, material released from the tributaries in the lower-middle reach of the estuary and from the coastal ocean has high potential to be transported to the upper estuary. The results reveal three distinct spatial patterns in the mainstem of an estuary for material released from different sources, namely, the main river input, tributary input, and coastal ocean input. Even though the Chesapeake Bay is selected as an example, the spatial pattern is applicable for other partially mixed estuary systems.

For the Chesapeake Bay, our results suggest that the main river (i.e., Susquehanna River) has dominant control on the concentration of riverine material in the mainstem and even in the lower reach of other tributaries through the bottom inflow in these subestuaries. Despite the small contribution from tributaries (e.g., Potomac, Rappahannock, York, and James Rivers), material from these rivers can be slowly moved to the upper estuary. The portion of materials moved to the upper estuary largely depends on the location of the tributary. Material from a tributary located near the mouth (e.g., James River) tends to have a relatively smaller portion of material transported to the upper Bay, due to the rapid flushing near the mouth area and the southward shelf current outside the mouth.

The spatial pattern illustrated by our simulation is not applicable to short-period release, which is highly subject to short-period events (e.g., hurricanes and storms). Further research on the event-driven transport is needed. Nevertheless, we hope that the general insights demonstrated by our numerical approach will help to improve the understanding of the source and fate of materials in estuarine and coastal systems.

Acknowledgments
We thank Mac Sisson for his assistance in editing the manuscript. We appreciate the anonymous reviewers for their constructive suggestions and comments on the manuscript. This work is supported by the National Science Foundation (award 1325518). Additional support is provided by Virginia Institute of Marine Science. The data sets used in this study have been made available at http://doi.org/10.5281/zenodo.570941. This is contribution No. 3679 of the Virginia Institute of Marine Science, College of William and Mary.

References

Anderson, D. M., Burkholder, J. M., Cochlan, W. P., Glibert, P. M., Gobler, C. J., Heil, C. A., … Parsons, M. L. (2008). Harmful algal blooms and eutrophication: Examining linkages from selected coastal regions of the United States. *Harmful Algae*, *8*(1), 39–53. https://doi.org/10.1016/j.hal.2008.08.017

Anderson, D. M., Stock, C. A., Keafer, B. A., Bronzino Nelson, A., Thompson, B., McGillicuddy, D. J., … Matrai, P. A. (2005). *Alexandrium fundyense* cyst dynamics in the Gulf of Maine. *Deep Sea Research*, *52*(19-21), 2522–2542. https://doi.org/10.1016/j.dsr2.2005.06.014

Austin, J. A. (2002). Estimating the mean ocean-bay exchange rate of the Chesapeake Bay. *Journal of Geophysical Research*, *107*, 3192. https://doi.org/10.1029/2001JC001246

Azevedo, I. C., Bordalo, A. A., & Duarte, P. M. (2010). Influence of river discharge patterns on the hydrodynamics and potential contaminant dispersion in the Douro estuary (Portugal). *Water Research*, *44*(10), 3133–3146. https://doi.org/10.1016/j.watres.2010.03.011

Baird, D., Ulanowicz, R. E., & Boynton, W. R. (1995). Seasonal nitrogen dynamics in Chesapeake Bay: A network approach. *Estuarine, Coastal and Shelf Science*, *41*(2), 137–162. https://doi.org/10.1006/ecss.1995.0058

Boynton, W. R., Garber, J. H., Summers, R., & Kemp, W. M. (1995). Inputs, transformations, and transport of nitrogen and phosphorus in Chesapeake Bay and selected tributaries. *Estuaries*, *18*(1), 285. https://doi.org/10.2307/1352640

Butt, A. J., L. C. Linker, J. S. Sweeney, G. W. Shenk, R. Batiuk, & C. Cerco (2000). Technical tools used in the development of Virginia's tributary strategies: A synthesis of airshed, watershed, and estuary model results. A Technical Summary Report. Richmond, VA: Department of Environmental Quality.

Caplow, T., Schlosser, P., Ho, D. T., & Santella, N. (2003). Transport dynamics in a sheltered estuary and connecting tidal straits: SF6 tracer study in New York Harbor. *Environmental Science & Technology*, *37*(22), 5116–5126. https://doi.org/10.1021/es034198+

Cerco, C. F., & Cole, T. (1993). Three-dimensional eutrophication model of Chesapeake Bay. *Journal of Environmental Engineering*, *119*(6), 1006–1025. https://doi.org/10.1061/(ASCE)0733-9372(1993)119:6(1006)

Cho, K. H., Wang, H. V., Shen, J., Valle-Levinson, A., & Teng, Y. (2012). A modeling study on the response of Chesapeake Bay to hurricane events of Floyd and Isabel. *Ocean Modelling*, *49-50*, 22–46. https://doi.org/10.1016/j.ocemod.2012.02.005

Cowan, J. L. W., & Boynton, W. R. (1996). Sediment-water oxygen and nutrient exchanges along the longitudinal axis of Chesapeake Bay: Seasonal pattern, controlling factors and ecological significance. *Estuaries*, *19*(3), 562–580. https://doi.org/10.2307/1352518

Dettmann, E. H. (2001). Effect of water residence time on annual export and denitrification of nitrogen in estuaries: A model analysis. *Estuaries*, *24*(4), 481. https://doi.org/10.2307/1353250

Du, J., & Shen, J. (2015). Decoupling the influence of biological and physical processes on the dissolved oxygen in the Chesapeake Bay. *Journal of Geophysical Research: Oceans*, *20*, 78–93. https://doi.org/10.1002/2014JC010422

Du, J., & Shen, J. (2016). Water residence time in Chesapeake Bay for 1980–2012. *Journal of Marine Systems*, *164*, 101–111. https://doi.org/10.1016/j.jmarsys.2016.08.011

Du, J., Shen, J., Bilkovic, D. M., Hershner, C. H., & Sisson, M. (2017). A numerical modeling approach to predict the effect of a storm surge barrier on hydrodynamics and long-term transport processes in a partially mixed estuary. *Estuaries and Coasts*, *40*(2), 387–403. https://doi.org/10.1007/s12237-016-0175-0

Epifanio, C. E., & Garvine, R. W. (2001). Larval transport on the Atlantic continental shelf of North America: A review. *Estuarine, Coastal and Shelf Science*, *51*, 51–77.

Festa, J. F., & Hansen, D. V. (1978). Turbidity maxima in partially mixed estuaries: A two-dimensional numerical model. *Estuarine and Coastal Marine Science*, *7*(4), 347–359. https://doi.org/10.1016/0302-3524(78)90087-7

Fortier, L., & Leggett, W. C. (1983). Vertical migration and transport of larval fish in a partially mixed estuary. *Canadian Journal of Fisheries and Aquatic Sciences*, *40*(10), 1543–1555. https://doi.org/10.1139/f83-179

Goodrich, D. M., & Blumberg, A. F. (1991). The fortnightly mean circulation of Chesapeake Bay. *Estuarine, Coastal and Shelf Science*, *32*(5), 451–462. https://doi.org/10.1016/0272-7714(91)90034-9

Guo, X., & Valle-Levinson, A. (2007). Tidal effects on estuarine circulation and outflow plume in the Chesapeake Bay. *Continental Shelf Research*, *27*(1), 20–42. https://doi.org/10.1016/j.csr.2006.08.009

Gustafsson, K. E., & Bendtsen, J. (2007). Elucidating the dynamics and mixing agents of a shallow fjord through age tracer modeling. *Estuarine, Coastal and Shelf Science*, *74*(4), 641–654. https://doi.org/10.1016/j.ecss.2007.05.023

Hamrick, J. M. (1992). A three-dimensional environmental fluid dynamics computer code: Theoretical and computational aspects. (Spec. Rep. 317). Gloucester Point, VA: Virginia Institute of Marine Science.

Hargis, W. J. (1980). A benchmark multi-disciplinary study of the interaction between the Chesapeake Bay and adjacent waters of the Virginian sea. In J. Campbell & J. Thomas (Eds.), *Chesapeake Bay Plume Study Superflux 1980*, *NASA Conference Publication* (Vol. 2188, pp. 1–14). Williamsburg, VA.

Hellweger, F. L., Blumberg, A. F., Schlosser, P., Ho, D. T., Caplow, T., Lall, U., & Li, H. (2004). Transport in the Hudson estuary: A modeling study of estuarine circulation and tidal trapping. *Estuaries*, *27*(3), 527–538. https://doi.org/10.1007/BF02803544

Hong, B., & Shen, J. (2012). Responses of estuarine salinity and transport processes to potential future sea-level rise in the Chesapeake Bay. *Estuarine and Coastal Marine Science*, *104-105*, 33–45. https://doi.org/10.1016/j.ecss.2012.03.014

Hong, B., & Shen, J. (2013). Linking dynamics of transport timescale and variations of hypoxia in the Chesapeake Bay. *Journal of Geophysical Research: Oceans*, *118*, 6017–6029. https://doi.org/10.1002/2013JC008859

Jiang, L., & Xia, M. (2016). Dynamics of the Chesapeake Bay outflow plume: Realistic plume simulation and its seasonal and interannual variability. *Journal of Geophysical Research: Oceans*, *121*, 1424–1445. https://doi.org/10.1002/2015JC011191

Kemp, W. M., Boynton, W. R., Adolf, J. E., Boesch, D. F., Boicourt, W. C., Brush, G., … Fisher, T. R. (2005). Eutrophication of Chesapeake Bay: Historical trends and ecological interactions. *Marine Ecology Progress Series*, *303*, 1–29. https://doi.org/10.3354/meps303001

Kemp, W. M., Sampou, P., Caffrey, J., Mayer, M., Henriksen, K., & Boynton, W. R. (1990). Ammonium recycling versus denitrification in Chesapeake Bay sediments. *Limnology and Oceanography*, *35*(7), 1545–1563. https://doi.org/10.4319/lo.1990.35.7.1545

Ko, F., & Baker, J. E. (2004). Seasonal and annual loads of hydrophobic organic contaminants from the Susquehanna River basin to the Chesapeake Bay. *Marine Pollution Bulletin*, *48*(9-10), 840–851. https://doi.org/10.1016/j.marpolbul.2003.10.014

Kuo, A. Y., & Neilson, B. J. (1987). Hypoxia and salinity in Virginia estuaries. *Estuaries*, *10*(4), 277–283. https://doi.org/10.2307/1351884

Lentz, S. J. (2008). Observation and a model of the mean circulation over the Middle Atlantic Bight continental shelf. *Journal of Physical Oceanography*, *28*, 1203–1221.

Levitus, S., Conkright, M. E., Reid, J. L., Najjar, R. G., & Mantyla, A. (1993). Distribution of nitrate, phosphate and silicate in the world oceans. *Progress in Oceanography*, *31*(3), 245–273. https://doi.org/10.1016/0079-6611(93)90003-V

Li, M., Zhong, L., Boicourt, W. C., Zhang, S., & Zhang, D. L. (2006). Hurricane-induced storm surges, currents and destratification in a semi-enclosed bay. *Geophysical Research Letters*, *33*, L02604. https://doi.org/10.1029/2005GL024992

Marshall, H. G., Egerton, T. A., Burchartdt, L., Cerbin, S., & Kokocinski, M. (2005). Long term monitoring results harmful algal populations in Chesapeake Bay and its major tributaries in Virginia, U.S.A. *Oceanological and Hydrobiological Studies*, *34*, 35–41.

Nixon, S. W., Ammerman, J. W., Atkinson, L. P., Berounsky, V. M., Billen, G., Boicourt, W. C., … Seitzinger, S. P. (1996). The fate of nitrogen and phosphorus at the land-sea margin of the North Atlantic Ocean. *Biogeochemistry*, *35*(1), 141–180. https://doi.org/10.1007/BF02179826

North, E. W., Schlag, Z., Hood, R. R., Li, M., Zhong, L., Gross, T., & Kennedy, V. S. (2008). Vertical swimming behavior influences the dispersal of simulated oyster larvae in a coupled particle-tracking and hydrodynamic model of Chesapeake Bay. *Marine Ecology Progress Series*, *359*, 99–115. https://doi.org/10.3354/meps07317

Oliveira, A., Fortunato, A. B., & Pinto, L. (2006). Modelling the hydrodynamics and the fate of passive and active organism in the Guadiana estuary. *Esutarine, Coastal and Shelf Science*, *70*(1-2), 76–84. https://doi.org/10.1016/j.ecss.2006.05.033

Park, K., Kuo, A. Y., Shen, J., & Hamrick, J. M. (1995). *A Three-Dimensional Hydrodynamic Eutrophication Model (HEM-3D): Description of water quality and sediment process submodels*, *Special Report in Applied Marine Science and Ocean Engineering* (Vol. 327, p. 102). Gloucester Point, VA: Virginia Institute of Marine Science.

Sanford, L. P., Suttles, S. E., & Halka, J. P. (2001). Reconsidering the physics of the Chesapeake Bay estuarine turbidity maximum. *Estuaries*, *24*(5), 655–669. https://doi.org/10.2307/1352874

Schubel, J. R., & Pritchard, D. W. (1986). Responses of upper Chesapeake Bay to variations in discharge of the Susquehanna River. *Estuaries*, *9*(4), 236–249. https://doi.org/10.2307/1352096

Scully, M. E. (2010). Wind modulation of dissolved oxygen in Chesapeake Bay. *Estuaries and Coasts*, *33*(5), 1164–1175. https://doi.org/10.1007/s12237-010-9319-9

Shen, J., Boon, J. D., & Kuo, A. Y. (1999). A modeling study of a tidal intrusion front and its impact on larval dispersion in the James River Estuary, Virginia. *Estuaries*, *22*(3), 681–692. https://doi.org/10.2307/1353055

Shen, J., & Gong, W. (2009). Influence of model domain size, wind directions and Ekman transport on storm surge development inside the Chesapeake Bay: A case study of extratropical cyclone Ernesto. *Journal of Marine Systems*, *75*(1-2), 198–215. https://doi.org/10.1016/j.jmarsys.2008.09.001

Shen, J., B. Hong, & A. Kuo (2013). Using timescales to interpret dissolved oxygen distributions in the bottom waters of Chesapeake Bay. *Limnology and Oceanography*, *58*(6), 2237–2248. https://doi.org/10.4319/lo.2013.58.6.2237

Shen, J., Hong, B., Schugam, L., Zhao, Y., & White, J. (2012). Modeling of polychlorinated biphenyls (PCBs) in the Baltimore Harbor. *Ecological Modelling*, *242*, 54–68. https://doi.org/10.1016/j.ecolmodel.2012.05.025

Shen, J., & Wang, H. V. (2007). Determining the age of water and long-term transport timescale of the Chesapeake Bay. *Estuarine, Coastal and Shelf Science*, *74*(4), 585–598. https://doi.org/10.1016/j.ecss.2007.05.017

Sinex, S. A., & Wright, D. A. (1988). Distribution of trace metals in the sediments and biota of Chesapeake Bay. *Marine Pollution Bulletin*, *19*(9), 425–431. https://doi.org/10.1016/0025-326X(88)90397-9

Skrabal, S. A. (1995). Distributions of dissolved titanium in Chesapeake Bay and the Amazon River Estuary. *Geochimica et Cosmochimica Acta*, *59*, 2449–2458.

Valle-Levinson, A., Reyes, C., & Sanay, R. (2003). Effects of bathymetry, friction, and rotation on estuary–ocean exchange. *Journal of Physical Oceanography*, *33*(11), 2375–2393. https://doi.org/10.1175/1520-0485(2003)033%3C2375:EOBFAR%3E2.0.CO;2

Valle-Levinson, A., Wong, K. C., & Bosley, K. T. (2001). Observations of the wind-induced exchange at the entrance to Chesapeake Bay. *Journal of Marine Research*, *59*(3), 391–416. https://doi.org/10.1357/002224001762842253

Voss, M., Bange, H. W., Dippner, J. W., Middelburg, J. J., Montoya, J. P., & Ward, B. (2013). The marine nitrogen cycle: Recent discoveries, uncertainties and the potential relevance of climate change. *Philosophical Transactions of the Royal Society of London. Series B: Biological Sciences*, *368*(1621), 20130121. https://doi.org/10.1098/rstb.2013.0121

Wong, K. C., & Valle-Levinson, A. (2002). On the relative importance of the remote and local wind effects on the subtidal exchange at the entrance to the Chesapeake Bay. *Journal of Marine Research*, *60*(3), 477–498. https://doi.org/10.1357/002224002762231188